

Freeform Body Motion Generation from Speech

Jing Xu¹ Wei Zhang² Yalong Bai² Qibin Sun¹ Tao Mei²

¹University of Science and Technology of China ²JD AI Research

xujing0@mail.ustc.edu.cn, wzhang.cu@gmail.com, ylbai@outlook.com,
qibinsun@ustc.edu.cn, tmei@live.com

Abstract

People naturally conduct spontaneous body motions to enhance their speeches while giving talks. Body motion generation from speech is inherently difficult due to the non-deterministic mapping from speech to body motions. Most existing works map speech to motion in a deterministic way by conditioning on certain styles, leading to sub-optimal results. Motivated by studies in linguistics, we decompose the co-speech motion into two complementary parts: pose modes and rhythmic dynamics. Accordingly, we introduce a novel freeform motion generation model (FreeMo) by equipping a two-stream architecture, i.e., a pose mode branch for primary posture generation, and a rhythmic motion branch for rhythmic dynamics synthesis. On one hand, diverse pose modes are generated by conditional sampling in a latent space, guided by speech semantics. On the other hand, rhythmic dynamics are synced with the speech prosody. Extensive experiments demonstrate the superior performance against several baselines, in terms of motion diversity, quality and syncing with speech. Code and pre-trained models will be publicly available through [URL](#).

1. Introduction

Body motion generation from speech is to synthesize spontaneous body motions synchronized with input speech audio. Professional speakers are experts in utilizing such motions to effectively deliver information. This task is essential for applications such as digital avatars and social robots. Notably with this technique, amateur speakers can also generate their own “professional” talking videos, by mimicking moves from professional speakers.

While generating lip motions has been extensively studied in talking heads generation [5], synthesizing plausible co-speech body motions remains an open issue. Specifically, lip motions can be well matched with the input audio using a deterministic mapping, i.e., one to one mapping

from phonemes¹ to lip shapes. However, such models can not be trivially extended to body, due to the highly stochastic nature of body motions during a talk speech. Practically, the co-speech body motion is highly *freeform*. Even if the same person gives the same speech twice in a row, there is no guarantee that the speaker would exhibit the same body motions. Moreover, a person usually switches poses from time to time during a long talking speech. As in Fig. 5, the same speech audio does not necessarily lead to a fixed form of motions, and different speeches may go well with the same motion sequence.

Most existing works treat body and lip motion generation in a similar way, i.e., the body landmarks are directly inferred from the input audio via a deep network [1, 6, 11, 19, 23, 31, 32]. To simplify the non-deterministic mapping, some methods rely on a set of pre-defined gestures [19], or condition on person-specific styles [11, 32] and templates [23]. These solutions can mimic motions of certain speakers/styles to some degree, but they are limited in terms of motion diversity and fidelity, especially for long talk speeches. Therefore, it is critical to develop algorithms that model the non-deterministic mapping between speech and body motions.

Based on studies in linguistics and psychology, co-speech motion helps the organization and presentation during speech delivery, and contributes in both semantics and intonation. Semantically, body motions guide the discourse organization (e.g., indicating topics and paragraphs), or contribute to the utterance content (e.g., describing shape using hands) [12]. For example, gesture change accompanying topic shifts better guide the audience into new topics [28]. Besides, some gestures are conventionalized and attached with certain linguistic properties (e.g., “thumbs up”). These gestures are widely used to facilitate communication. In terms of intonation, the rhythmic movement that matches to the prosody of audio could attract attentions of the audience, with the stressed syllable during speech. Moreover, proper rhythmic motions² also reflect the progress of the

¹Basic elements of speech audio.

²Also called beat gestures in some literature.

speech and deliver a vivid listening experience [8,26]. Such co-speech motion usually has no specific linguistic meaning, and manifests as simple and fast hand dynamics related to the prosody [20].

Motivated by these studies, we consider the structure of co-speech motions in a novel perspective. We introduce the concept of *pose mode* as the mode of the pose distribution that speakers has for fragments of speech. Considering the speaker’s posture in a speech video as a random vector, it follows a multi-modal distribution in the high dimensional space. Modes in such distribution (values with local maximal density) corresponds to conventionalized gestures or the habitual postures of speakers. Our work focuses on motions in talk videos, where speakers organize a long speech around a certain topic. Under this setting, the pose modes are mostly habitual postures with no specific global meaning. Consequently, the structure of co-speech motions can be considered as the sequential transitions of *pose modes* with *rhythmic dynamics* under each pose mode. Therefore, the non-deterministic mapping from speech to body motion is decomposed into two parts: a stochastic mapping from speech semantics to pose modes, and the mapping from speech prosody to rhythmic motion dynamics. Our contributions are summarized as follows:

- To address the non-deterministic mapping from speech to body motions, we propose to decompose the motion into pose modes and rhythmic motions. The former is stochastically generated with conditional sampling in a VAE latent space, and the latter is effectively inferred by speech prosody.
- Extensive experiments demonstrate that our model generates plausible freeform motions well synced with the speech, outperforming other baselines in terms of diversity, quality and syncing with clear margin.

2. Related Work

2.1. Relation between Speech and Body Motion

According to studies in linguistics and gesture [12], there are two main functions of co-speech body motions, namely *substantial* and *pragmatic* gestures. The former one contributes to the speech content (e.g., hands are better suited to describe shapes), while the latter one contributes to the situational embedding such as conveying attitudes or agreement or guiding the discourse organization. Besides, beat gestures manifest simple and fast movements of the hands. Rather than directly conveying meaning, they are synchronized with prosodic events in speech and contribute to the perceiving of the speech and function in the sense of audio-visual prosody [26].

2.2. Co-speech Motion Generation

Rule-based. Rule-based methods rely on pre-defined mapping to generate appropriate body motions. Most approaches rely on a fixed set of gesture templates, and operate on text inputs [15]. A typical solution is to associate each word to a gesture [3]. Further improvements include assigning synchronization points [21], or analysing communicative goals [14].

Learning-based. While learning-based methods are successful on lip motion generation [6, 10, 22, 27, 31], the application on co-speech motion generation is far from mature. Previous methods typically treat co-speech body and lip motions in a similar way. However, talking head generation [6,31] mostly predicts facial motions in a deterministic mapping. Recent methods model co-speech motion generation as a sequence-to-sequence translation problem. For example, recurrent neural networks [33] are adopted to generate motions from a speech transcript. Speech2gesture [11] uses 1D fully-convolutional networks to map speech to motion sequences. Trimodal-context [32] takes both text and audio as input, and synthesizes body motions using recurrent networks. However, these methods learn a deterministic mapping from speech to motion, while essentially this mapping is non-deterministic.

3. Freeform Co-speech Motion Generation

Co-speech body motion generation is to generate the corresponding motion sequence, according to a given speech audio. To this end, a mapping from speech to body motion is required. Unfortunately, such mapping is highly non-deterministic and multi-modal. We approach this problem by decomposing the body motion into two complementary parts: pose modes and rhythmic dynamics. Correspondingly, our framework consists of two branches: a pose mode branch and a rhythmic motion branch, as shown in Fig. 1.

3.1. Framework Overview

Given a piece of speech audio S and the corresponding body motion M , co-speech motion generation is to establish the mapping: $S \rightarrow M$. Without loss of generality, in this work, S and M are represented as MFCC [24] feature and human pose landmarks [9, 16, 29], respectively. To ease discussion, S and M are chunked into clips with small duration, i.e., $S = [S_1, S_2, \dots, S_n]$, and $M = [M_1, M_2, \dots, M_n]$, where each $S_i \in \mathbb{R}^{T \times D_S}$ or $M_i \in \mathbb{R}^{T \times D_M}$ corresponds to T consecutive frames in the talk videos. D_S and D_M indicate the feature dimension of audio and motion respectively. With the Markov assumption, the problem turns to learn the mapping from (S_i, M_{i-1}) to M_i .

Learning such mapping is non-trivial due to the non-deterministic nature. Motivated by studies in linguistics and behavior [8, 12, 20, 26, 28], we decompose the body motions

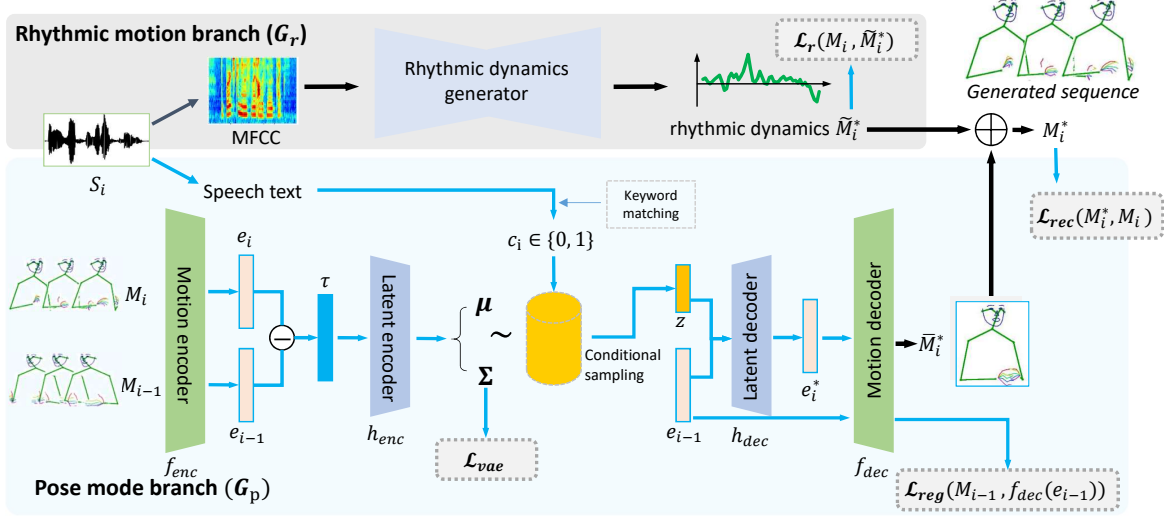


Figure 1. The framework of our freeform co-speech motion generation model (FreeMo) during training. The whole framework consists of two branches, a rhythmic motion branch that learns the mapping from speech audio to rhythmic dynamics, and a pose mode branch which is constructed as a CVAE by conditional sampling based on semantic signals in speech text to generate free-form pose modes.

M_i into two parts:

$$M_i = \bar{M}_i + \tilde{M}_i, \quad (1)$$

where \bar{M}_i encodes the primary pose mode, and \tilde{M}_i embeds the rhythmic dynamics of M_i . Accordingly, our framework is composed with two major branches, where the pose mode branch (G_p) controls the primary postures (\bar{M}_i), conditioning on the audio S_i and last step motion M_{i-1} :

$$\bar{M}_i^* = G_p(M_{i-1}, S_i), \quad (2)$$

and the rhythmic motion branch (G_r) is responsible for the rhythmic dynamics (\tilde{M}_i) synced with the speech prosody:

$$\tilde{M}_i^* = G_r(S_i). \quad (3)$$

We put a superscript (*) to denote the generated results. With such decomposition, the pose mode branch is only responsible for the pose mode generation, and the rhythmic motion branch learns the rhythmic dynamics independent to the primary pose.

3.2. Pose Mode Generation

During a talk speech, the speakers' primary postures are mostly habitual and have no conventionalized linguistic meaning. We do not apply specific constraints on the forms of pose modes, but introduce a conditioning sampling trick to switch among learned pose modes.

We first introduce a label $c_i \in \{0, 1\}$ to indicate whether there is a pose mode change from M_{i-1} to M_i , and then learn a latent space to generate transitions among pose

modes. Conditioning on c_i , the generated \bar{M}_i^* either keeps the pose of last step, or transits into a new one. Specifically, a conditional variational autoencoder (CVAE) is introduced, whose latent space encodes the modes transition between training pairs (M_{i-1}, M_i) given c_i .

Following the convention [30], the transition feature can be represented as the difference of encoded motions:

$$\tau = e_i - e_{i-1}, \quad (4)$$

where $e_i = f_{enc}(M_i)$, $e_{i-1} = f_{enc}(M_{i-1})$, and f is the motion encoder network. The VAE encoder (h_{enc}) takes τ as the input and calculates the posterior distribution as $\mathcal{N}(\mu_\theta(\tau), \Sigma_\theta(\tau))$. The VAE decoder takes the sampled vector $z \sim \mathcal{N}(\mu_\theta(\tau), \Sigma_\theta(\tau))$ and e_{i-1} to recover e_i^* , which is then decoded as $\bar{M}_i^* = f_{dec}(e_i^*)$.

VAE Latent Loss. A VAE loss is introduced for conditional sampling. For each training sample $\{M_{i-1}, M_i, S_i\}$, c_i indicates whether there is a pose mode switch at time i . Ideally, c_i is closely related to the semantics (e.g., topic shifts) of speech. Practically, this can also be pseudoly labeled by calculating the extent of hand position change between M_{i-1} and M_i . When $c_i = 1$ (with pose change), we minimize the KL divergence between estimated posterior distribution $\mathcal{N}(\mu_\theta(\tau), \sigma_\theta(\tau))$ and the prior $\mathcal{N}(\mathbf{0}, \mathbf{I})$ [13], as M_{i-1} and M_i are with different modes:

$$\mathcal{L}_1 = KL(\mathcal{N}(\mu_\theta(\tau), \sigma_\theta(\tau)) || \mathcal{N}(\mathbf{0}, \mathbf{I})). \quad (5)$$

When $c_i = 0$ (without pose change), we use a zero vector as the latent transition representation z for all training samples (with $c_i = 0$), that is, $e_i^* = h_{dec}(\mathbf{0}, e_{i-1})$. To keep

the consistency of the latent encoder and latent decoder, we introducing the following constraint:

$$\mathcal{L}_0 = \|\mu_\theta(\tau)\| + \|\Sigma_\theta(\tau)\|. \quad (6)$$

Note that while M_i and M_{i-1} are in a same pose modes, they may have different rhythmic dynamics. Mapping all such samples into a same latent representation makes the encoder ignore the differences in rhythmic dynamics but focus on pose modes. The complete VAE latent loss can be written as:

$$\mathcal{L}_{vae} = \mathbb{I}(c_i = 0)\mathcal{L}_0 + \mathbb{I}(c_i = 1)\mathcal{L}_1. \quad (7)$$

Regularizing the embedding space. Our pose mode branch is formulated as a conditional motion prediction. However, only deterministic data samples are available for training (for each M_{i-1} , the subsequent M_i is fixed). As a result, the latent code z can be easily ignored, and the model degenerates to deterministic prediction, i.e., $\overline{M}_i^* = f_{dec}(h_{dec}(z, e_{i-1})) \rightarrow \overline{M}_i^* = f_{dec}(e_{i-1})$, where h_{dec} is the VAE decoder. We regularize the embedding space of the motion encoder f and the motion decoder g as:

$$\mathcal{L}_{reg} = \|M_i - f_{dec}(e_i)\| + \|M_{i-1} - f_{dec}(e_{i-1})\|. \quad (8)$$

This prevents the motion decoder g from ignoring the latent code z and basing its predictions on e_{i-1} .

3.3. Rhythmic Motion Generation

Besides the primary posture, the temporal dynamics of the body motion is also an essential part in speech-motion correlation [26]. The rhythmic dynamics in co-speech motions are simple and fast movements driven by the prosodic events in speech, contributing to the perceived prominence of temporally aligned speech and the sense of audiovisual prosody. We introduce the rhythmic motion branch to further match the dynamics with the speech prosody. In this work, we use a convolutional network as the rhythmic dynamics generator.

Rhythmic motion loss. The rhythmic motion branch learns the rhythmic dynamics (\widetilde{M}_i^*) independent to the primary poses. The corresponding loss function is defined as:

$$\mathcal{L}_r = \left\| \widetilde{M}_i^* - (M_i - M_i^m) \right\|, \quad (9)$$

where M_i^m is the arithmetic mean of motions in M_i (over T frames). \mathcal{L}_r ensures the generated result \widetilde{M}_i^* with the proper offset to the mean posture, which helps control the motion dynamics without affecting the primary posture. To verify this effect, we conduct a test to swap the primary posture and rhythmic dynamics as shown in Fig. 2. Given two motion sequences M_A and M_B , we exchange their motion dynamics as $M_A^* = M_A^m + (M_B - M_B^m)$ and

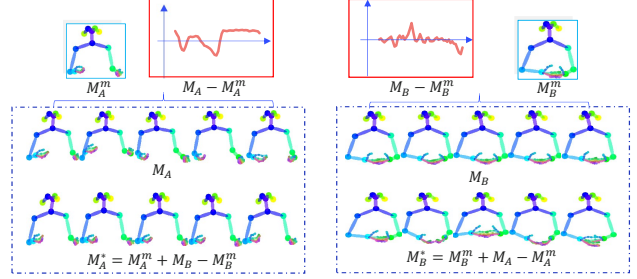


Figure 2. Disentangling rhythmic dynamics and primary posture in body motions. M_A and M_B are two random motion sequences sampled from our training set. The red boxes denote the offset to the mean posture of the motion sequence. We can control the motion dynamics without affecting the primary postures by exchanging the offset in the motion sequences. See supplement files for better temporal illustration.

$M_B^* = M_B^m + (M_A - M_A^m)$. As shown, while the motion dynamics are exchanged, the principle postures in M_A and M_B are preserved in M_A^* and M_B^* , and the motion fidelity is not affected.

3.4. Overall Loss Function

We apply the reconstruction loss on the final result $M_i^* = \overline{M}_i^* + \widetilde{M}_i^*$:

$$\mathcal{L}_{rec} = \|M_i^* - M_i\|. \quad (10)$$

Overall, the loss function is summarized as:

$$\mathcal{L} = \lambda_1 \mathcal{L}_{rec} + \lambda_2 \mathcal{L}_{vae} + \lambda_3 \mathcal{L}_r + \lambda_4 \mathcal{L}_{reg}, \quad (11)$$

where $\lambda_1 \sim \lambda_4$ are the balancing weights for each loss.

3.5. Inference Pipeline

During inference, the pose mode branch implements the following function:

$$\overline{M}_i^* = G_p(M_{i-1}^*, S_i) = f_{dec}(h_{dec}(z, e_{i-1})), \quad (12)$$

where z is a randomly sampled vector conditioned on c_i , and c_i is inferred from the speech text in S_i (e.g., with keyword matching). Specifically, when $c_i = 0$, z is a zero vector encoding the mode transitions where M_{i-1} and M_i are in a same pose mode; when $c_i = 1$, z is randomly sampled from $\mathcal{N}(\mathbf{0}, \mathbf{1})$, encoding the mode transition of training samples where M_{i-1} and M_i are in different pose modes. The final generation result for the whole input speech S is the temporal stack of the generated motions at each step $[M_1^*, M_2^*, \dots, M_n^*]$, where $M_i^* = \overline{M}_i^* + \widetilde{M}_i^*$.

4. Experimental Results

4.1. Experimental Setup

Datasets. Following the convention [1, 11, 23], we also test on the the *Speech2Gesture* dataset [11], which contains speaker-specific videos of Television anchors. However, most videos are TV shows with heavy interference from the environment (e.g., sound from audience, front desk), and the body motions are constrained as the speakers often seat in chairs or lean against desks (Fig. 3).

Therefore, we include another *Ted Gesture* dataset [33] to evaluate on videos of keynote talks. Following the setting as in [11], we add more videos collected from YouTube to ensure enough data for each speaker. We split these segments as 80% for training, 10% for testing, 10% for validation. Fig. 3 shows some snapshots of *Speech2Gesture* and *TEDGesture*.

Compared Methods. We compare with the following state-of-the-art methods:

- Audio to Body Dynamics (Audio2Body) [25] adopts an RNN network for audio to motion translation.
- Speech2Gesture (S2G) [11] proposes a convolutional network for speech to gesture generation.
- Speech Drives Template (Tmpt) [23] learns a set of gesture templates to relieve the ambiguity of the mapping from speech to body motion.
- Trimodal-Context (TriCon) [32] adopts an RNN network that takes (audio, text, speaker) triplet as input. Speaker ID specifies the styles for generated motions.
- Mix-StAGE [1] learns a unique style embedding for each speaker using a mixture of generation models.

Evaluation Protocol. Co-speech motion generation is essentially a non-deterministic prediction task, as multiple motion sequences are plausible for a same speech audio. Metrics that only evaluate against one ground-truth motion (e.g., $L1$ loss [11]) are somewhat biased. In this work, three quantitative metrics [18] are considered for evaluating the generated motions: 1) *syncing* between speech and motion, 2) *diversity* of motions, and 3) *quality* of motions as compared to real ones. Besides, qualitative comparison and user study are included as subjective evaluations.

4.2. Quantitative Results

Syncing. The synchronization between generated motions and speech is one of the most essential factors indicating how well the model captures the relation of speech and motion. Landmark velocity difference (LVD) [35] is adopted to evaluate the syncing with speech, as we do not expect to generate motions exactly the same as the ground-truth.



Figure 3. Example videos in *Speech2Gesture* dataset (top) and *TEDGesture* dataset (bottom).

Tables 1 and 2 show the LVD scores of different models on *TEDGesture* and *Speech2Gesture* datasets, respectively. For completeness, we also include two direct data-driven baselines [30]: 1) *Last-step Velocity* that uses the initial velocity of the ground-truth motion as the prediction; 2) *Mean Velocity* that uses the average velocity of the ground-truth motion sequence as the prediction. Note that *Mean Velocity* is actually a strong baseline, when comparing the LVD between ground-truth and generated motions.

As shown, FreeMo outperforms other baselines, suggesting better syncing ability in relating audio and motion. Our model shows strong performances on all speakers as evidenced by the low LVD scores, while other baselines fail to sync on some speakers. Our model is more robust to different speaker styles, leading to lower averaged LVD scores. Note that the absolute LVD scores on *Speech2Gesture* are smaller than those on *TEDGesture*, since body motions in *Speech2Gesture* are much simpler and static (Fig. 3).

Diversity and Quality. We further evaluate our method in terms of diversity and quality. Specifically, we measure the diversity by calculating the average distances among 64 motion sequences generated from a same initial posture for each test audio. To measure the quality (fidelity) of generated motions, we train a binary classifier to discriminate real samples from fake ones and use the prediction score on the test set as the quality of the generated motions [2].

Table 3 shows the comparison results of diversity and quality on different methods. S2G, Mix-StAGE, Tmpt, Audio2Body and TriCon are all essentially based on deterministic models. Therefore the diversity is not applicable, i.e., fixed output for the same input. Our FreeMo reaches a diversity of 0.163 due to the conditional sampling technique. As a comparison, if we manually set different style inputs for TriCon to generate diverse motions, the diversity score reaches 0.193, which is slightly higher than our FreeMo.

The quality of our model is much better than all baselines, mimicking moves similar to real speakers. This demonstrates the ability to generate both diverse and plausible co-speech motions, which can also be observed in our user study. Note that better syncing leads to degenerated diversity, and these scores are better jointly considered.

	Amel	Bill	Christina	Dan	Dena	Enric	Kelly	Keller	Sara	Stanley	Average↓
Last-step Velocity	15.9	34.0	26.3	21.9	20.8	13.5	17.6	21.3	14.9	17.9	20.4
Mean Velocity	16.1	12.8	10.7	15.9	11.4	14.1	11.2	11.4	12.0	10.8	12.6
Audio2Body [25]	23.7	18.6	19.8	23.0	27.8	20.1	21.5	23.0	19.3	22.4	21.9
TriCon [32]	16.6	16.5	20.2	13.7	16.0	13.8	11.5	13.6	14.1	11.0	14.7
S2G [11]	12.8	11.3	19.4	22.0	12.2	11.9	10.6	10.7	11.8	10.0	13.3
Mix-StAGE [1]	11.8	16.0	9.9	16.5	9.4	10.5	17.3	11.4	12.2	14.7	13.0
Tmpt [23]	14.6	11.5	10.1	13.7	13.3	10.9	10.7	11.6	11.9	12.3	12.1
FreeMo (ours)	11.7	11.4	9.2	12.7	8.0	9.7	10.4	10.3	11.0	9.0	10.3

Table 1. Quantitative comparison on *TEDGesture* dataset for syncing between speech and motions using LVD (lower is better). The best and second results are marked in red and blue, respectively.

	Almaram	Angelica	Chemistry	Ellen	Oliver	Seth	Shelly	Average↓
Last-step Velocity	17.5	16.6	11.1	18.5	17.4	19.2	33.1	19.1
Mean Velocity	10.3	7.4	6.1	9.0	7.2	5.1	16.1	8.7
Audio2Body [25]	14.5	23.1	8.3	10.0	14.1	11.5	17.1	14.1
TriCon [32]	8.6	9.3	5.2	7.8	5.7	4.1	13.8	7.8
S2G [11]	11.4	5.5	4.4	8.6	5.2	3.9	11.3	7.2
Mix-StAGE [1]	11.2	11.8	4.7	9.6	11.9	9.2	15.7	10.6
Tmpt [23]	9.6	6.2	4.9	7.9	5.3	4.2	13.1	7.3
FreeMo (ours)	7.6	5.6	4.8	6.8	5.5	4.3	12.4	6.7

Table 2. Quantitative comparison on *Speech2Gesture* dataset for syncing between speech and motions using LVD (lower is better). The best and second results are marked in red and blue, respectively.

Method	Diversity↑	Quality↑
Audio2Body [25]	NA	0.375
S2G [11]	NA	0.163
Mix-StAGE [1]	NA	0.382
Tmpt [23]	NA	0.178
TriCon [32]	NA	0.278
FreeMo (ours)	0.160	0.502

Table 3. Quantitative evaluation on the quality and diversity. *NA*: the method essentially learns a deterministic mapping and thus diversity is not applicable.

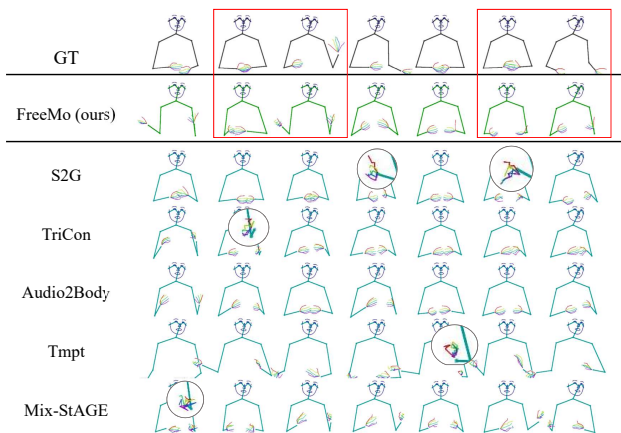


Figure 4. Qualitative comparisons on co-speech motion generation results. We highlight the unrealistic hand deformations appeared in the baseline methods. We also outline the pose changes in red boxes to show the expressiveness of our method. See supplementary material for more video results.

4.3. Qualitative Results

Fig. 4 shows the qualitative comparisons across different models. Motions generated by the baseline methods contain hand deformations, while such deformations can hardly be found in our model. Intuitively, motions generated by S2G and TriCon typically are small movements around a certain

posture. They lack clear pose transitions as appeared in the ground-truth (outlined in the red boxes), leading to less realistic and expressive motions. Such movements are difficult to synthesize through the direct audio to motion mapping. Motions by Audio2Body show noisy dynamics and poor temporal continuity. Compared to these methods, our FreeMo generates more natural and expressive motions.

A common problem for co-speech motion generation is the severe jittering, which can be observed in almost all baselines (see supplementary file for temporal consistency). They directly translate speech to motion sequence, and thus the audio-conditioned dynamics and the primary postures are coupled and simultaneously inferred from the audio. Benefiting from the decomposition, our model has much stable generation quality.

To demonstrate the high diversity of our model, we provide multiple generation results of our model for the same speech in Fig. 5, including motions generated from a same initial posture and different initial postures. Our model generates diverse motion sequences from an arbitrary initial posture. It is worth noting that we do not rely on different initialization to obtain diverse results. This is achieved by the stochastic mode transitions of the pose mode branch. In the red boxes we highlight the transitions of pose modes. At each transition, the generated posture has a large degree of freedom, while the occurrences of transitions are synchronized with the ground-truth. Besides, the rhythmic branch

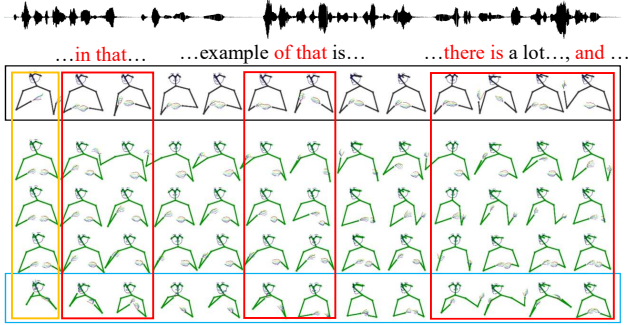


Figure 5. Multiple motion sequences for a same speech generated by our model. The red boxes highlight the occurrences of pose mode transitions in the generated motions and the ground-truth motions (first row). See supplementary material for video results.

	TEDGesture	Speech2Gesture
Audio2Body [25]	2.09	2.11
TriCon [32]	2.36	2.89
S2G [11]	2.81	3.28
Tmpt [23]	4.09	4.55
Mix-StAGE [1]	3.91	3.11
FreeMo	5.73	5.05

Table 4. Subjective user study on two datasets. The participants are asked to rank the videos generated by different models according to their preferences from highest (6) to lowest (1). Each row shows the averaged user preference rank for each method.

plays a critical role in syncing the generated motion with the speech, such that the dynamics of generated sequence match well to the audio.

4.4. Subjective Evaluation

We further conduct subjective user study to evaluate the user preferences against several baselines. For each dataset, we randomly select 50 test audio clips. These audio clips are of different lengths from 10s to 30s. The participants are asked to rank the videos generated by different models according to their preferences from highest (6) to lowest (1). Ten participants attended in this user study, each of them watches the videos for 10 randomly chosen audio clips. Table 4 reports the average preference scores. We can see that on both datasets, our proposed FreeMo has highest scores, preferred by most users. According to the participants’ feedback, their decisions are mostly influenced by three aspects: 1) visual fidelity, e.g., hand deformations, motion continuity and speed; 2) the syncing to special prosodic events, such as emphasis, turning point in the speech; 3) motion expressiveness, e.g., motions with large and concise movements are preferred, while motions with small (or static) movements are less favored.

\mathcal{L}_r	\mathcal{L}_{reg}	multi-speaker	Syncing↓	Diversity↑	Quality↑
✗	✓	✗	10.8	0.202	0.582
✓	✗	✗	10.6	0.125	0.583
✓	✓	✗	10.3	0.160	0.502
✓	✓	✓	10.2	0.254	0.375

Table 5. Ablation study results on our FreeMo. *multi-speaker* stands for training on multiple speakers simultaneously. These speakers are from a held-out set excluding speakers in the test set.

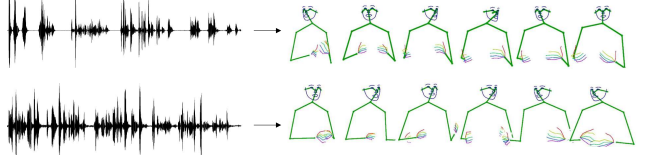


Figure 6. Same model on different audio. We select audios with different prosody, and compare the generation results of a same model on these audios.

4.5. Ablation Study

We further run an ablation study on the losses (\mathcal{L}_r , \mathcal{L}_{reg}). Note that \mathcal{L}_{rec} can not be removed for proper training, and removing \mathcal{L}_{vae} degenerates the model to a deterministic mapping [11].

As shown in Table 5, removing \mathcal{L}_r results in a worse syncing score. This is expected as the syncing of the posture transitions are preserved, while the dynamics of the generated sequences no longer match to the audio. The diversity and quality are higher than the full model, since the generated motions are less constrained and their rhythmic dynamics resemble the training samples. The generated motions for a same speech audio are also less similar to each other due to the worse syncing ability. Removing \mathcal{L}_{reg} leads to a decline in diversity and syncing, as the model becomes more deterministic. These results also demonstrate that for co-speech motion generation, both semantics and prosody of the audio should be considered.

4.6. Discussion on Cross-ID Generation

For applications such as social robots and digital avatar, the driving audio usually are synthesized or recorded by voice actors. It is unlikely to train speaker-specific models for each speaker. Therefore, the generalization ability to different speakers is highly desired. Therefore we further analyze the performance on audio of unseen speakers.

Same model on different audio. The generalization ability to unseen speakers essentially reflects that the model generates body motions based on ID-independent speech features, such as semantics, intonation, etc., rather than overfit to ID-specific features such as timbre. To show this, we select audios from different speakers and compare the generation results by a fixed model. As shown in Fig. 6, for

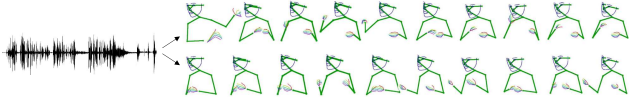


Figure 7. The generation results of different model on a same audio. While these models are trained on data of different speakers and they generate body motions with different postures, the generated motion dynamics are similar.

speech with low speed, the model generates soothing body movements. When the speed is faster, the movements will also be faster.

Different models on the same audio. Most existing works map speech to motion via conditioning on personal styles. Contrary to this, we do not attempt to fit the personal style of individual speakers. While different speakers may have their own styles, their motions contribute to the speech generally in a similar way [28]. The generated sequences for a same audio by different models are shown in Fig. 7. While these models are trained on different speakers and they generate body motions with different postures, the generated motion dynamics are roughly similar. This shows that our model captures the essential correlation between speech and motion that is shared across speakers.

Training on multiple speakers. The distribution of training data is critical to the generalization ability of deep learning models. However, the speech videos of a single speaker is very limited, due to personal habits. It is difficult to train a model with strong generalization ability using videos from a single speaker. Therefore, it is important to use data from different speakers to construct sufficient training data. To explore this, we use ten extra speakers videos as the training set. The results are shown in the last row of Table 5. The trained model has a comparable performance in syncing compared to the speaker-specific models (the third row in Table 5), and much better diversity. Our model successfully transits between the pose modes learnt from multiple speakers, showing highly diverse motions. Fig. 8 shows the original video frames of the nearest neighbors of postures in the generated sequence. There are multiple habitual postures of different speakers appearing in the same generation result. The posture style of different speakers are jointly modeled by our model, enabling higher generalization diversity. The lower quality score might be caused by the out-of-distribution problem, i.e., the extra ten speakers are not included while training the quality classifier.

4.7. Video Rendering

We further show the RGB video rendering results based on our generated motions, as depicted in Fig. 9. We adopt a similar approach as in [4] for video generation. The video results can be end-to-end synthesized given an input speech audio. Interestingly, we can render the generated motions

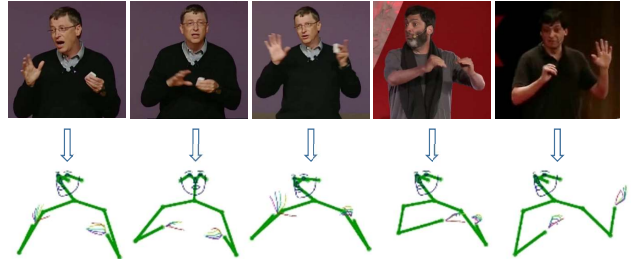


Figure 8. The original video frames of the nearest neighbors of the postures in the generated sequence trained on multi-speakers. The posture styles of different speakers are combined in a same generation result.

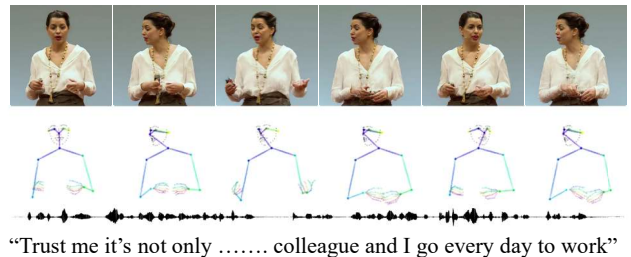


Figure 9. The end-to-end rendering video results. From bottom to top row: speech text, speech audio, generated motion sequence, rendered video frames.

based on arbitrary identities, which enables applications such as generating “professional” speech videos for amateur speakers by mimicking moves of professional speakers.

5. Conclusion and Discussion

In this work, we propose the FreeMo for co-speech motion generation. Motivated by studies in linguistics and psychology, we address the non-deterministic mapping by decomposing the hard task into complementary parts. Given an input speech audio, the pose mode branch sequentially generates diverse pose modes with conditional sampling, and the rhythmic motion branch concurrently enriches each pose mode with audio-conditional rhythmic dynamics for spontaneous motions. Our model generates highly diverse and visually plausible body motions in a freeform manner.

Open Issues. Our method is based on 2D skeleton landmarks that lack kinetics constrains. Thus current form is sensitive to severe body shape deformations (i.e., bone length). Possible solutions may include adopting a 3D model to represent body and its motion (M). Moreover, as we do not consider full spectrum of semantic postures, our model is limited in handling the substantial gestures [12] that convey conventionalized semantic meaning (e.g., greetings). A sound solution is to incorporate pre-defined semantic gestures [19] into the pipeline.

Broader impact. This work helps build virtual agents to relieve human labor, which is essential for applications such as social robots adopted in Robotics and digital avatars prevalent in Metaverse. Also, there is possibility towards abused fake video generation. Right now, the negative impact is limited, since this technique is far from mature, not to mention the extensive works on identifying computer generated contents [7, 17, 34].

References

- [1] Chaitanya Ahuja, Dong Won Lee, Yukiko I Nakano, and Louis-Philippe Morency. Style transfer for co-speech gesture animation: A multi-speaker conditional-mixture approach. In *European Conference on Computer Vision*, pages 248–265. Springer, 2020. 1, 5, 6, 7
- [2] Sadegh Aliakbarian, Fatemeh Sadat Saleh, Mathieu Salzmann, Lars Petersson, and Stephen Gould. A stochastic conditioning scheme for diverse human motion prediction. In *Proceedings of the IEEE/CVF Conference on Computer Vision and Pattern Recognition*, pages 5223–5232, 2020. 5
- [3] Justine Cassell, Hannes Högni Vilhjálmsson, and Timothy Bickmore. Beat: the behavior expression animation toolkit. In *Life-Like Characters*, pages 163–185. Springer, 2004. 2
- [4] Caroline Chan, Shiry Ginosar, Tinghui Zhou, and Alexei A Efros. Everybody dance now. In *Proceedings of the IEEE/CVF International Conference on Computer Vision*, pages 5933–5942, 2019. 8
- [5] Lele Chen, Guofeng Cui, Ziyi Kou, Haitian Zheng, and Chenliang Xu. What comprises a good talking-head video generation?: A survey and benchmark. *arXiv preprint arXiv:2005.03201*, 2020. 1
- [6] Lele Chen, Guofeng Cui, Celong Liu, Zhong Li, Ziyi Kou, Yi Xu, and Chenliang Xu. Talking-head generation with rhythmic head motion. In *European Conference on Computer Vision*, pages 35–51. Springer, 2020. 1, 2
- [7] Zhikai Chen, Lingxi Xie, Shanmin Pang, Yong He, and Bo Zhang. Magdr: Mask-guided detection and reconstruction for defending deepfakes. In *Proceedings of the IEEE/CVF Conference on Computer Vision and Pattern Recognition*, pages 9014–9023, 2021. 9
- [8] Paul Ekman and Wallace V Friesen. Hand movements. *Journal of communication*, 22(4):353–374, 1972. 2
- [9] Hao-Shu Fang, Shuqin Xie, Yu-Wing Tai, and Cewu Lu. RMPE: Regional multi-person pose estimation. In *ICCV*, 2017. 2
- [10] Ohad Fried, Ayush Tewari, Michael Zollhöfer, Adam Finkelstein, Eli Shechtman, Dan B Goldman, Kyle Genova, Zeyu Jin, Christian Theobalt, and Maneesh Agrawala. Text-based editing of talking-head video. *ACM Transactions on Graphics (TOG)*, 38(4):1–14, 2019. 2
- [11] Shiry Ginosar, Amir Bar, Gefen Kohavi, Caroline Chan, Andrew Owens, and Jitendra Malik. Learning individual styles of conversational gesture. In *Proceedings of the IEEE/CVF Conference on Computer Vision and Pattern Recognition*, pages 3497–3506, 2019. 1, 2, 5, 6, 7
- [12] Adam Kendon. *Gesture: Visible action as utterance*. Cambridge University Press, 2004. 1, 2, 8
- [13] Diederik P Kingma and Max Welling. Auto-encoding variational bayes. *arXiv preprint arXiv:1312.6114*, 2013. 3
- [14] Stefan Kopp and Ipke Wachsmuth. Synthesizing multimodal utterances for conversational agents. *Computer animation and virtual worlds*, 15(1):39–52, 2004. 2
- [15] Sergey Levine, Philipp Krähenbühl, Sebastian Thrun, and Vladlen Koltun. Gesture controllers. In *ACM SIGGRAPH 2010 papers*, pages 1–11. 2010. 2

- [16] Jiefeng Li, Can Wang, Hao Zhu, Yihuan Mao, Hao-Shu Fang, and Cewu Lu. Crowdpose: Efficient crowded scenes pose estimation and a new benchmark. *arXiv preprint arXiv:1812.00324*, 2018. 2
- [17] Lingzhi Li, Jianmin Bao, Ting Zhang, Hao Yang, Dong Chen, Fang Wen, and Baining Guo. Face x-ray for more general face forgery detection. In *Proceedings of the IEEE/CVF Conference on Computer Vision and Pattern Recognition*, pages 5001–5010, 2020. 9
- [18] Ruilong Li, Shan Yang, David A Ross, and Angjoo Kanazawa. Ai choreographer: Music conditioned 3d dance generation with aist++. In *Proceedings of the IEEE/CVF International Conference on Computer Vision*, pages 13401–13412, 2021. 5
- [19] Miao Liao, Sibozhang, Peng Wang, Hao Zhu, Xinxin Zuo, and Ruigang Yang. Speech2video synthesis with 3d skeleton regularization and expressive body poses. In *Proceedings of the Asian Conference on Computer Vision*, 2020. 1, 8
- [20] David McNeill. *Gesture and thought*. University of Chicago press, 2008. 2
- [21] Isabella Poggi, Catherine Pelachaud, Fiorella de Rosis, Valeria Carofiglio, and Berardina De Carolis. Greta. a believable embodied conversational agent. In *Multimodal intelligent information presentation*, pages 3–25. Springer, 2005. 2
- [22] KR Prajwal, Rudrabha Mukhopadhyay, Vinay P Namboodiri, and CV Jawahar. A lip sync expert is all you need for speech to lip generation in the wild. In *Proceedings of the 28th ACM International Conference on Multimedia*, pages 484–492, 2020. 2
- [23] Shenhan Qian, Zhi Tu, Yihao Zhi, Wen Liu, and Shenghua Gao. Speech drives templates: Co-speech gesture synthesis with learned templates. In *Proceedings of the IEEE/CVF International Conference on Computer Vision*, pages 11077–11086, 2021. 1, 5, 6, 7
- [24] Md Sahidullah and Goutam Saha. Design, analysis and experimental evaluation of block based transformation in mfcc computation for speaker recognition. *Speech communication*, 54(4):543–565, 2012. 2
- [25] Eli Shlizerman, Lucio Dery, Hayden Schoen, and Ira Kemelmacher-Shlizerman. Audio to body dynamics. In *Proceedings of the IEEE Conference on Computer Vision and Pattern Recognition*, pages 7574–7583, 2018. 5, 6, 7
- [26] Michael Studdert-Kennedy. Hand and mind: What gestures reveal about thought. *Language and Speech*, 37(2):203–209, 1994. 2, 4
- [27] Supasorn Suwajanakorn, Steven M Seitz, and Ira Kemelmacher-Shlizerman. Synthesizing obama: learning lip sync from audio. *ACM Transactions on Graphics (TOG)*, 36(4):1–13, 2017. 2
- [28] Petra Wagner, Zofia Malisz, and Stefan Kopp. Gesture and speech in interaction: An overview, 2014. 1, 2, 8
- [29] Yuliang Xiu, Jiefeng Li, Haoyu Wang, Yinghong Fang, and Cewu Lu. Pose Flow: Efficient online pose tracking. In *BMVC*, 2018. 2
- [30] Xinchen Yan, Akash Rastogi, Ruben Villegas, Kalyan Sunkavalli, Eli Shechtman, Sunil Hadap, Ersin Yumer, and Honglak Lee. Mt-vae: Learning motion transformations to generate multimodal human dynamics. In *Proceedings of the European Conference on Computer Vision (ECCV)*, pages 265–281, 2018. 3, 5
- [31] Ran Yi, Zipeng Ye, Juyong Zhang, Hujun Bao, and Yongjin Liu. Audio-driven talking face video generation with learning-based personalized head pose. *arXiv preprint arXiv:2002.10137*, 2020. 1, 2
- [32] Youngwoo Yoon, Bok Cha, Joo-Haeng Lee, Minsu Jang, Jaeyeon Lee, Jaehong Kim, and Geehyuk Lee. Speech gesture generation from the trimodal context of text, audio, and speaker identity. *ACM Transactions on Graphics (TOG)*, 39(6):1–16, 2020. 1, 2, 5, 6, 7
- [33] Youngwoo Yoon, Woo-Ri Ko, Minsu Jang, Jaeyeon Lee, Jaehong Kim, and Geehyuk Lee. Robots learn social skills: End-to-end learning of co-speech gesture generation for humanoid robots. In *2019 International Conference on Robotics and Automation (ICRA)*, pages 4303–4309. IEEE, 2019. 2, 5
- [34] Hanqing Zhao, Wenbo Zhou, Dongdong Chen, Tianyi Wei, Weiming Zhang, and Nenghai Yu. Multi-attentional deepfake detection. In *Proceedings of the IEEE/CVF Conference on Computer Vision and Pattern Recognition*, pages 2185–2194, 2021. 9
- [35] Yang Zhou, Xintong Han, Eli Shechtman, Jose Echevarria, Evangelos Kalogerakis, and Dingzeyu Li. Makeltalk: speaker-aware talking-head animation. *ACM Transactions on Graphics (TOG)*, 39(6):1–15, 2020. 5